ORIGINAL ARTICLE

A revolutionary acute subdural hematoma detection based on two-tiered artificial intelligence model

İsmail Kaya, M.D.,[1] Tuğrul Hakan Gençtürk, M.D.,[2] Fidan Kaya Gülağız, M.D.[2]

[1]Department of Neurosurgery, Niğde Ömer Halisdemir University, Faculty of Medicine, Niğde-*Türkiye*
[2]Department of Computer Engineering, Kocaeli University, Faculty of Engineering, Kocaeli-*Türkiye*

ABSTRACT

BACKGROUND: The article was planned to make the first evaluation in terms of acute subdural hemorrhages, thinking that it can help in appropriate pathologies by tomography interpretation with the artificial intelligence (AI) method, at least in a way to quickly warn the responsible doctor.

METHODS: A two-level AI-based hybrid method was developed. The proposed model uses the mask-region convolutional neural network (Mask R-CNN) technique, which is a deep learning model, in the hemorrhagic region's mask generation stage, and a problem-specific, optimized support vector machines (SVM) technique which is a machine learning model in the binary classification stage. Furthermore, the bee colony algorithm was used for the optimization of SVM algorithms' parameters.

RESULTS: In the first stage, the mean average precision (mAP) value was obtained as 0.754 when the intercept over union (IOU) value was taken as 0.5 with the Mask R-CNN architecture used. At the same time, when a 5-fold cross-validation was applied, the mAP value was obtained 0.736. With the hyperparameter optimization for both Mask R-CNN and the SVM algorithm, the accuracy of the two-level classification process was obtained as 96.36%. Furthermore, final false-negative rate and false-positive rate values were obtained as 6.20%, and 2.57%, respectively.

CONCLUSION: With the proposed model, both the detection of hemorrhage and the presentation of the suspicious area to the physician were performed more successfully on two dimensional (2D) images with low cost and high accuracy compared to similar studies and today's interpretations with telemedicine techniques.

Keywords: Acute subdural hematoma; artificial intelligence; early diagnosis.

INTRODUCTION

Since 1967, when Sir Godfrey Hounsfield discovered computed tomography (CT), it has been an indispensable method for rapid-acting pathology determination, especially in cranial pathologies.[1,2] It is the most important imaging tool used in emergency pathologies such as bone fractures, cranial hemorrhages, midline shifts, masses especially hemorrhagic and calcified ones, edema, hydrocephalus, hemorrhagic infarcts, and late isolated infarcts.[2] Compared to MRI (magnetic resonance imaging), CT has no alternative due to its advantages such as no long-term immobility requirement, no need for respirators with special magnetic properties especially for intubated patients, useful in claustrophobic patients, and obtainable from patients with metal body implants.[3,4] In addition, it is important that CT can be obtained quickly in seconds from mobile organs, as well as patients who are urgent and incompatible.[3] Although it is necessary to be careful in sensitive populations since it contains X-ray radiation, thanks to today's developing technologies, radiation exposure has been minimized.[5] It can be obtained cheaply due to the use of X-ray technology, which has been widely used since 1895 and has become widespread rapidly.[6,7] In the USA, even ambulances with mobile tomography were built for early

Cite this article as: Kaya İ, Gençtürk TH, Kaya Gülağız F. A revolutionary acute subdural hematoma detection based on two-tiered artificial intelligence model. Ulus Travma Acil Cerrahi Derg 2023;29:858-871.

Address for correspondence: İsmail Kaya, M.D.
Niğde Ömer Halisdemir University, Faculty of Medicine, Niğde, Türkiye
E-mail: hekimikaya@gmail.com

Ulus Travma Acil Cerrahi Derg 2023;29(8):858-871 DOI: 10.14744/tjtes.2023.76756 Submitted: 03.10.2022 Revised: 22.03.2023 Accepted: 23.04.2023

stroke diagnosis.[8] With 1035 CT devices today, it is available throughout Türkiye.[9] Thus, it is accessible to the level of the major township and widespread.[9]

All this current situation has caused new threats. In places where specialist physicians are not available, the presence of tomography has created the need for CT images' interpretation by general practitioners. Practitioners, especially those who carry the burden of emergency wards, had to interpret the whole-body tomography. In the current education system, this ability is out of the curriculum even among emergency specialist doctors'.[10,11] It imposes responsibilities on doctors that they cannot handle. Furthermore, due to legal requirements in current practice, it is expected that the radiology doctor will report the CT images separately usually with telemedicine, even in urgent patients.[12] Thus, if patients are not met with a very experienced doctor, it causes diagnosis and treatment delays.[12]

In recent years, developing technology has led to advances in many areas, as well as enabling us to perform operations in the field of artificial intelligence (AI) that we could not imagine before. AI basically refers to the ability to simulate tasks that require intelligence by machines.[13] Machine learning and deep learning methods, whose popularity is increasing day by day, are also sub-branches of AI.[13] Machine learning deals with how machines can extract useful information from data.[14] Deep learning is a machine learning sub-branch (Fig. 1).[14] In both categories, the techniques have different advantages over each other.[14] The learning process is faster in machine learning techniques compared to deep learning techniques, but they require the feature extraction process.[14] Deep learning techniques also work with long training times, but they automate the feature extraction process.[14] Furthermore, deep learning techniques are more successful on much larger data.[14] At the same time, deep learning techniques can also be processed with numeric or non-categorical data types such as sound and image.[14] There is a need for techniques that use these two AI sub-branches as a hybrid, especially in cases where the data set is unstable and inputs/outputs other than numeric/categorical types should be used.[14] CT images used in the diagnosis of diseases in the field of health are also one of the areas where these hybrid techniques can be useful.

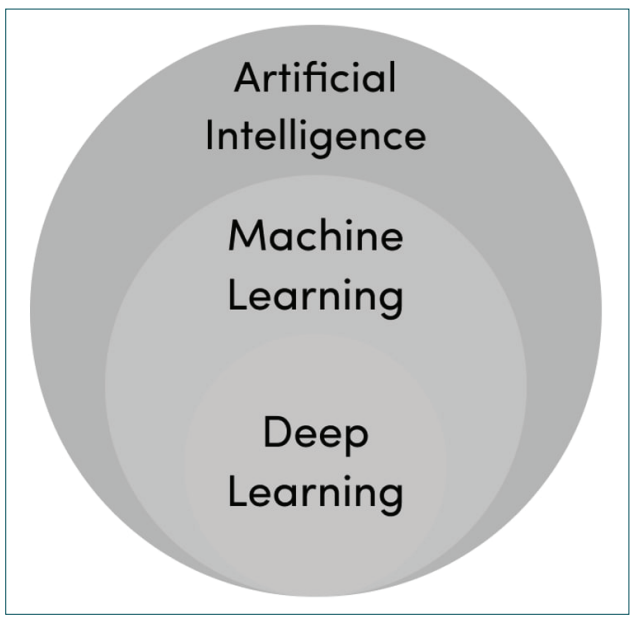

Figure 1. Artificial intelligence, machine learning, and deep learning coverage.

Considering all this information, this article was planned to make the first evaluation in terms of acute subdural hemorrhages (ASDH), thinking that it can help in appropriate pathologies by filling the gap, we mentioned in the tomography interpretation with the AI method, at least in a way to quickly warn the responsible doctor. For this purpose, this study tried to examine ASDH detection with a two-level model that uses both machine learning and deep learning techniques. The proposed model uses the mask-region convolutional neural network (Mask R-CNN) technique, which is a deep learning model, in the hemorrhagic region's mask generation stage, and a problem-specific, optimized support vector machines (SVM) model, which is a binary classification stage machine learning technique. The work as such is original and unique.

MATERIALS AND METHODS

The data to be used for the study were obtained by collecting ASDH cases followed up and treated by Assistant Professor İsmail KAYA at Niğde Ömer Halisdemir University Faculty of Medicine Neurosurgery Clinic and at Cumhuriyet University Faculty of Medicine Neurosurgery Clinic. AI studies were carried out by uploading anonymized digital imaging and communications in medicine (DICOM) extension images to the server under the control of Kocaeli University Faculty of Engineering Assistant Professor Fidan KAYA GÜLAĞIZ and graduate student Tuğrul Hakan GENÇTÜRK. The server has an i7 4790K 8 Core CPU, 24 GB RAM, and 6 GB graphics card. The server connection was made with secure and closed system architecture, allowing only the researchers' IP (Internet Protocol) addresses.

Within the AI studies' scope, firstly data labeling was carried out by Assistant Professor İsmail KAYA and controlled. At this stage, CVAT (Computer Vision Annotation Tool) software was used. Before marking, sample images with DICOM extension were converted to portable network graphics (png) extension (Fig. 2). With the polygon marking technique, the masks of the hemorrhagic areas were generated. Allocating these masks, the data set planned to be used for the segmentation problem was created. The evaluation process of the two-level model is explained in the following steps.

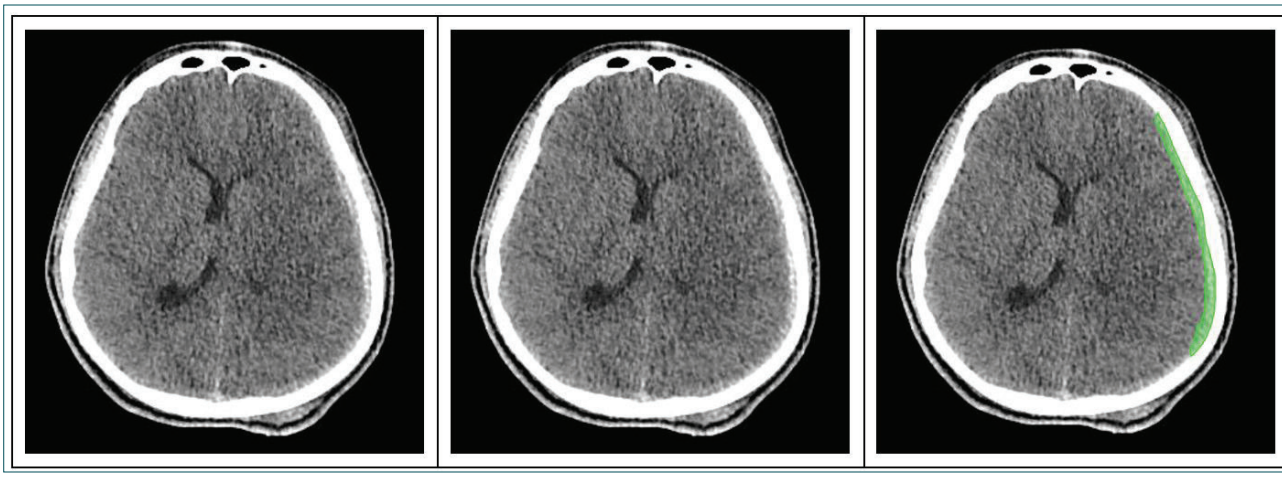

Figure 2. (a) DICOM image, (b) Png Image, and (c) image with the marked bleeding area.

- Step 1: Separation of data as training and testing
- Step 2: Creation of segmentation model using training data
- Step 3: Evaluation of the segmentation model using test data
- Step 4: Implementation of the classification model (At this stage, four different models were evaluated.).
  a. Classification using only segmentation model outputs
  b. Classification by averaging the Hounsfield unit value of the segmentation outputs
  c. Classification by giving the features of the segmentation outputs to the Liner SVM
  d. Classification by giving the features of the segmentation outputs to the SVM radial basis function (RBF).
- Step 5: Obtaining the classification success of the two-level model over the test data.

As explained in Step 1, labeled data (831 images in total) were randomly divided into 80% training (686 images) and 20% testing (145 images). During this separation process, the patient images used as test data were not mixed with the training data. In Step 2, segmentation of suspected hemorrhagic regions was performed using Mask R-CNN model with a residual neural network 50 (ResNet-50) - feature pyramid network (FPN) backbone. In Step 3, the model was evaluated on the test data, and the model's segmentation success was obtained. In addition, to evaluate the model's average success over the data set, a 5-fold cross-validation was also made in the segmentation process. In Step 4, for the second level, the classification process was carried out using the result directly from the Mask R-CNN algorithm without extracting additional features first. Then, the average HU value of the pixels that belonged to the segmented region was calculated. Only the HU value was used as the threshold for binary classification. The case of this minimum threshold HU value ≥45–50 were evaluated separately and binary classification results were obtained for all threshold values. The case of maximum threshold HU value was accepted 80 for all. While determining the HU threshold value, the standard values were considered.[15] It has been noticed that if the threshold value is used plainly, some hemorrhagic areas cannot be detected correctly. To increase the method's success, asymmetry index, mean value, standard deviation, kurtosis, skewness, and the length ratio values of the sides in the *x*, and *y* axes of the box drawn around the hemorrhagic area were obtained over the HU value. These data were transformed into feature vectors and given as the SVM model input. At this stage, first, the classical linear SVM model was preferred. RBF kernel and Artificial Bee Colony algorithm were used to optimize the model specific to the problem. For the training of the SVM algorithm, 365 non-hemorrhagic images taken from four new patients were segmented with the Mask R-CNN model. Although there were no hemorrhages in 64 of these images, Mask R-CNN made incorrect segmentation. Sixty-four images with incorrect segmentation were labeled as non-hemorrhagic. From the hemorrhagic images used in the first-level train phase, 135 images taken from randomly selected patients were added. Thus, for the SVM algorithm, a new training set was created. This training set's features were obtained with the SVM algorithm. Then, to determine the model's success, all the test data consisted of first-level hemorrhagic images (145 images) and non-hemorrhagic images of four new patients (350 images) segmented with Mask R-CNN were given. With the SVM algorithm used at the second level, it was possible to determine whether the areas labeled as suspicious by Mask R-CNN at the first level were hemorrhage or not.

Mask R-CNN is a region-based convolutional neural network (CNN) used for instance segmentation. It outputs the masks of the objects as well as the bounding boxes and the confidence score. With Mask R-CNN, the segmentation algorithm was run by Open multimedia laboratory, and the SVM algorithm was run with the scikit-learn library. The Mask R-CNN model used in the first level utilized png extension CT images (512 × 512 size) as input and gave masks of suspicious regions as output. Mask R-CNN consists of two stages. The first stage consists of two networks, which are a feature extraction network (Residual Network, Inception.) called the backbone and a region bidding network. The used

Mask R-CNN model's backbone consists of ResNet-50 and FPN (Fig. 3). These meshes run once per image to suggest a region range. Region suggestions were regions that contain the feature map's object. In the second step, for each of the suggested regions obtained in Step 1, the neural network predicted the bounding boxes and object class. Not every proposed region had to be the same size, but fully connected layers in networks always required a fixed-size vector. Using the region of interest (RoI) pool or the RoI-Align method, the recommended regions were sized to fully connected layers.

ResNet50 architecture, which forms the Mask R-CNN basis, has several stages (Fig. 4). Each ResNet architecture performs initial convolution and maximum pooling using 7 × 7 and 3 × 3 kernels, respectively. In the network's Phase 1, there are three constructive blocks, each containing three layers. In all three layers of the Phase 1 block, the cores' size used to perform the convolution is 64, 64, and 256, respectively. As you move from one stage to the next the channel width is doubled, and the input size is halved. Using 1 × 1 kernels in a top-down approach with the FPN network, the ResNet architecture output is converted into feature maps. The FPN extracts feature maps and then feeds these to the region proposal network (RPN) for object detection. RPN implements a floating window over feature maps to make predictions

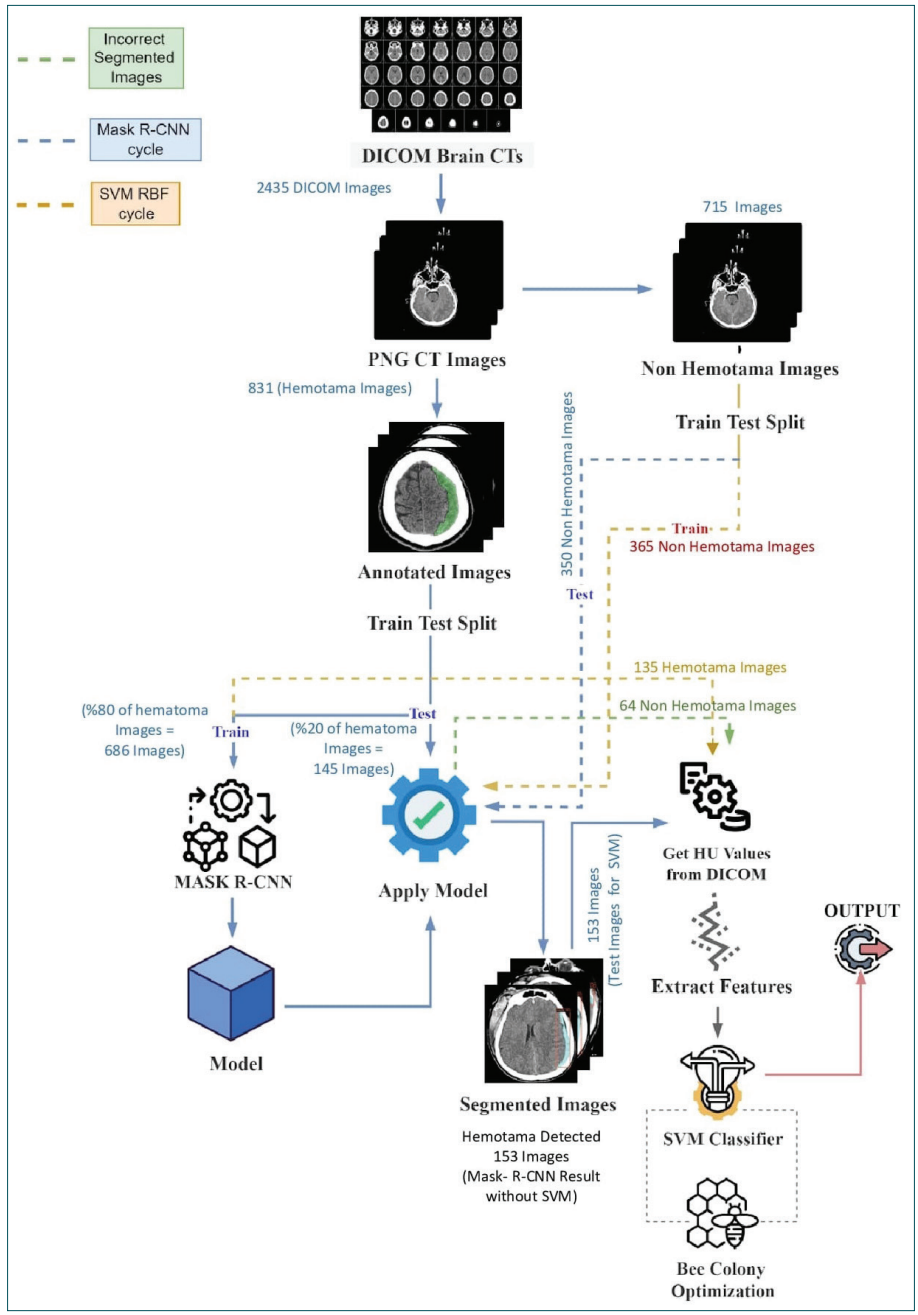

Figure 3. General system architecture.

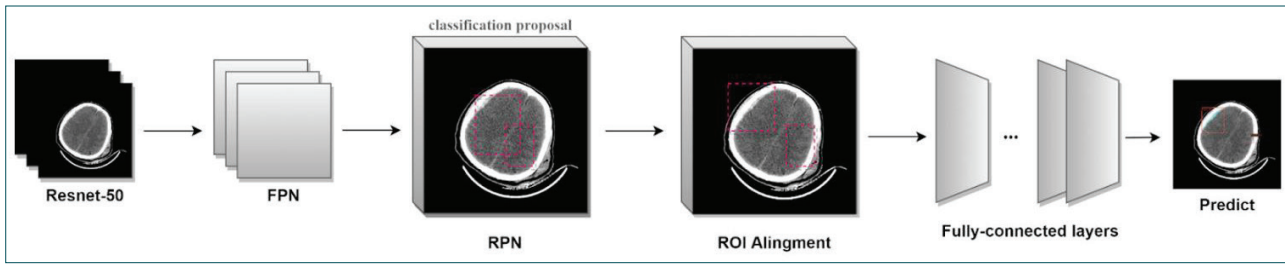

Figure 4. Mask R-CNN architecture.

about object boundary boxes at target locations. On each feature map generated by the FPN network, 3 × 3 convolution kernels are applied, followed by 1 × 1 kernels for object predictions and bound box regression.

Hyperparameter optimization is a key step to obtain problem-specific models. In the SVM algorithm, c and gamma are the most important hyperparameters. The c hyperparameter was used to control the model's error, while the gamma parameter was used to control the curve's boundary in nonlinear classifications. Therefore, these two hyperparameters determined the classification performance specific to our model. Within the scope of the study, the bee colony algorithm was used for the optimization of these parameters.

After the model optimization was completed, an open dataset CQ500[16] was used to generalize the model. In the CQ500 dataset, there are 53 scans, and 6391 slices belong to these scans containing SDH.[16] The model proposed in the article aims to detect ASDH. For this reason, a total of 76 slices containing only ASDH in the CQ500 dataset were used. The CQ500 dataset does not contain ground truth segmentation masks. Therefore, before training, these slices were converted to png format and later marked to obtain masks. Sixty of the png images were added to the previously used training data and 16 of them were added to the test data. After that, the training and testing of the model have performed again.

During the classification process' evaluation, the F1 score value and the accuracy value were used together. The mean average precision (mAP) metric, which was calculated by taking the intercept over union (IOU) value of 0.5, was used to determine the hemorrhagic region's segmentation accuracy.

RESULTS

Within the scope of the study, 2434 CT images were collected from 26 patients. Of these, 831 images had an ASDH. Although age and gender were not important for tomography data, 27% of the patients evaluated were female and 73% were male (seven females and 19 males). The minimum age of the patients included was 3 years, and the maximum age was 85 years (with median age was 43 years and mean age was 40.5 years), respectively. The patient distribution was similar to the age and sex ratios were seen in ASDHs in the community.[17,18] In the first stage, images with hemorrhage were randomly divided into 80% training and 20% testing. After this segmentation process, the mAP value was obtained as 0.754 when the IOU value was taken as 0.5 with the Mask R-CNN architecture used. At the same time, when a 5-fold cross-validation was applied, the mAP value was 0.736. In Figure 5, the segmentation process' sample images are shared.

Simultaneously, 715 images of eight new non-hemorrhagic patients were used to train the second stage SVM model and evaluated the overall success of the proposed two-level model. Of these, 365 images of four patients were used in the SVM model training, and the remaining 350 images were used in the architecture evaluation. When binary classification was performed using only the Mask R-CNN algorithm, the accuracy value was obtained as 95.15%. When the HU value was added to the classification, 94.55% and 92.93% binary classification successes were obtained for the threshold HU values of 45 and 50, respectively. In the last stage, when the features obtained from the HU value were used, the method's success for the linear SVM algorithm was determined as 94.95%.

Gamma and c values[19] giving the highest accuracy were obtained as 0.0708 and 12.2844, respectively. The gamma and c hyper parameters' variation of the Artificial Bee Colony algorithm used to optimize the SVM algorithm is shown visually in Figure 6 and numerically in Table 1. In the figure, the X-axis represents the iteration number of the algorithm, and the Y-axis represents the accuracy value corresponding to these iterations. Since the SVM algorithm performs to reduce the loss value, there is an inverse relationship between the loss value and the accuracy. For this reason, the accuracy value is given with a "-" sign. In terms of the classification process, the highest accuracy value is 1. In the figure, the best value obtained with the SVM algorithm is shown with the blue line, and the mean values depending on the iterations are shown with the red dots. With the hyperparameter optimization for both Mask R-CNN and the SVM algorithm, the final accuracy of the two-level classification process was obtained as 96.36%.

In the proposed two-level model's evaluation, in addition to the accuracy value, the F1 score value which gives the average of the precision and recall values was also taken into consideration. The accuracy, precision, recall, and F1 score values of all techniques used during the model's development are

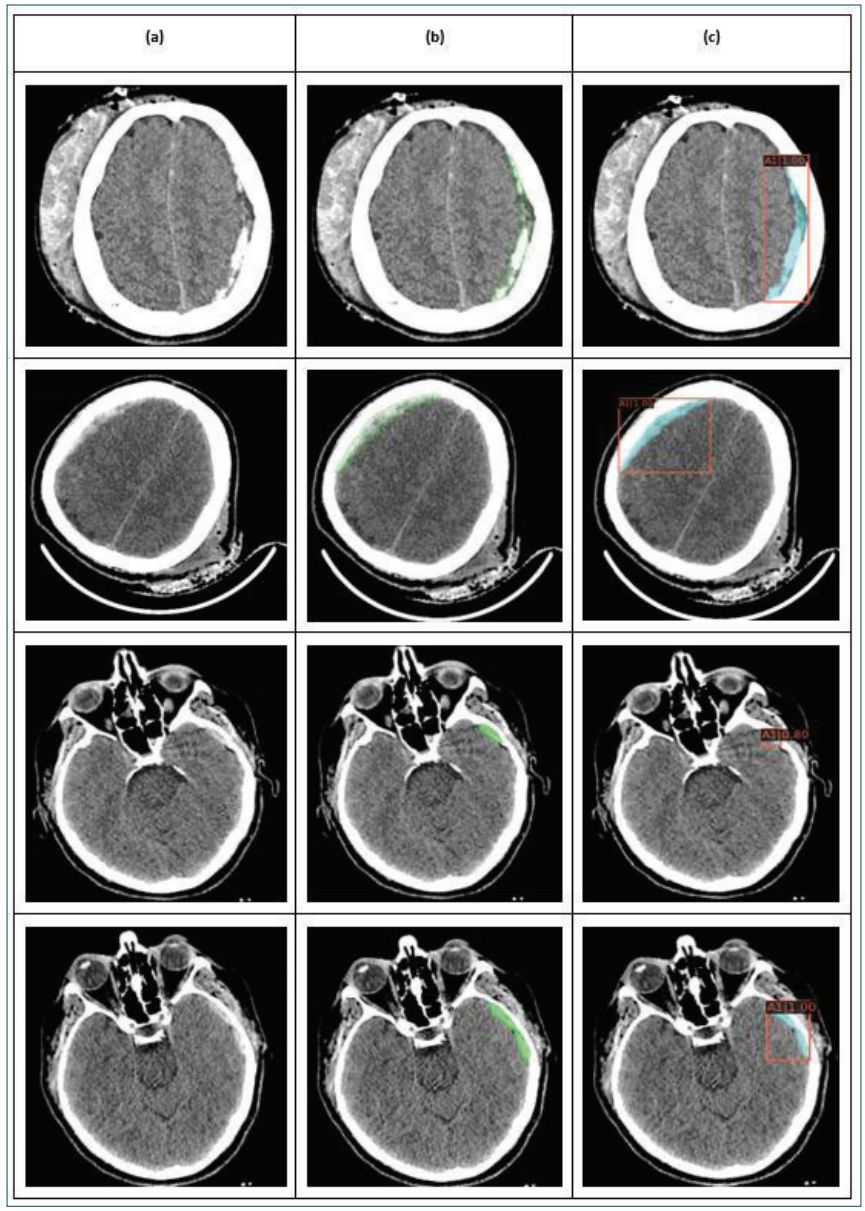

Figure 5. Sample segmentation result (a): Image with unmarked bleeding, (b): Image marked by neurosurgeon, and (c): Image marked by Mask R-CNN algorithm.

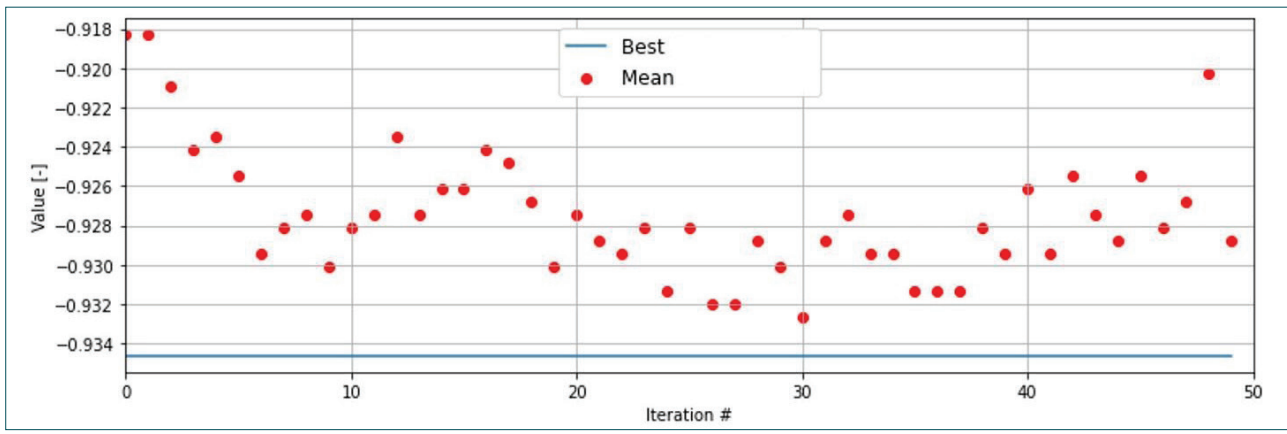

Figure 6. Relation between SVM hyperparameters and classification accuracy.

Table 1. Relation between gamma and C parameter and classification accuracy

Gamma	C	Accuracy*
0.0430	29.6389	91,50
0.0430	35.4891	91,50
0.0430	39.2157	91,50
0.0544	35.4891	92,81
0.0708	**12.2844**	**93,46**
0.0708	**34.0026**	**93,46**
0.0708	**34.5049**	**93,46**
0.0943	7.4010	90,85
0.0943	7.4454	90,85
0.0985	7.4010	90,85

*It is given as a percentage (%)

shown with detail in Table 2. Furthermore, negative predictive value (NPV), false-negative rate (FNR), and false-positive rate (FPR) metrics were calculated. The NPV value, which was detecting the absence of hemorrhage in the study, expressed by the model's class 1, was calculated as 95.43% when the classification was made over the Mask R-CNN model only, and as 97.43% when the recommended two-level model was used. Within the study's scope, FNR represents the rate of images that was estimated to be absent when hemorrhage was present, and FPR represents the rate of images in which hemorrhage was detected when there was no hemorrhage. [19] When classification was made only with the Mask R-CNN model, the FNR value was found as 10.45% and the FPR value as 2.33% whereas, the proposed two-level model used specified values were determined as 6.20% and 2.57%, respectively.

When we evaluated with the expanded data set (our data + slices having only ASDH in CQ500), for the first level of the model, the accuracy of Mask R-CNN was obtained as 93.93%

Table 2. Binary classification results for different algorithms

	Accuracy*	Precision	Recall	F1 Score
Without hounds field value (only mask R-CNN)				
Class 1 (No hematoma)	95.15	0.95	0.98	0.97
Class 2 (Hematoma)	95.15	0.94	0.90	0.92
Hounds Field Value (Threshold 45)				
Class 1 (No hematoma)	94.55	0.96	0.96	0.96
Class 2 (Hematoma)	94.55	0.91	0.90	0.91
Hounds Field Value (Threshold 50)				
Class 1 (No hematoma)	92.93	0.96	0.94	0.95
Class 2 (Hematoma)	92.93	0.85	0.90	0.88
Linear SVM				
Class 1 (No hematoma)	94.95	0.99	0.95	0.97
Class 2 (Hematoma)	94.95	0.86	0.96	0.91
SVM with RBF				
Class 1 (No hematoma)	96.36	0.97	0.97	0.97
Class 2 (Hematoma)	96.36	0.94	0.94	0.94

*It is given as a percentage (%)

Table 3. Segmentation and binary classification results with extended dataset

	Accuracy*	Precision	Recall	F1 Score
Only mask R-CNN				
Class 1 (No hematoma)	93.93	0.91	0.99	0.95
Class 2 (Hematoma)	93.93	0.99	0.84	0.95
SVM with RBF				
Class 1 (No hematoma)	95.30	0.94	0.99	0.96
Class 2 (Hematoma)	95.30	0.98	0.88	0.93

*It is given as a percentage (%)

and with the RBF based SVM algorithm, the accuracy of the two-level classification process was obtained as 95.30%. In Table 3, the results obtained on the expanded data set are given for binary classification.

DISCUSSION

Traumatic brain injury is one of the most important health problems worldwide.[20] Today, it is ever-growing exponentially with increasing mobilization and population density.[20] For head trauma, CT is the most effective diagnostic method.[2] It is widely and inexpensively available today.[2] Especially in emergency pathologies, this situation places the responsibility of evaluating the whole-body CT scans on our general practitioners and specialist doctors. In the current curriculum, this subject is not taught holistically in both medical education and specialist doctorate education.[10,11] Although it is taught as scattered, radiology specialist reports are needed.[12] Today, these reports are made through e-medicine with a subcontractor model and have high false report rates.[21] In places where experienced doctors are not available, the current status causes serious delays in emergency pathologies, thus increasing mortality and morbidity.[22] We think that the status quo can change with AI. Previously, there were similar problems in interpreting electrocardiography devices' reports, and by simple automated reporting using primitive calculation methods, most of the problem has been solved.[23] However, tomography images that require advanced image processing and AI cannot be reported in this way.[14] The subject was discussed parallel with the developments in recent years again.[13] With our original method, we achieved better results than e-medicine applications in every parameter as described above.[21,22]

Within the study's scope, a two-level model that combines both machine learning and deep learning technique advantages have been proposed for the detection of ASDHs. The proposed model performs the segmentation process with the MASK R-CNN architecture at the first level, and the classification process at the second level with the SVM architecture developed specifically for the problem. It is known that the MASK R-CNN method was used in segmentation problems using medical images and gave successful results.[24-28] The elimination of areas labeled as hemorrhagic due to artifacts, as a result of the segmentation process performed at the first level, was achieved by the SVM algorithm used at the second level. If the average of the HU value was used alone, the model was more affected by the errors that may occur during the hemorrhagic area marking (marking the areas of the bone, cavity, artifact, etc.). For this reason, instead of using the HU value alone, we gave different features such as standard deviation and asymmetry obtained from this value as the SVM algorithm input used in the classification phase. When the feature space is small and the features contain statistical data, the SVM algorithm gives superior results.[29,30] In the second level of the study, the features used were statistical values, and the feature space was also six-dimensional. For these reasons, the SVM algorithm was preferred. Furthermore, different techniques such as random forest, Naive Bayes, and Multilayer Perceptron have been tested within the study's scope, but due to the data size, these algorithms have not been as successful as much as SVM. When problem-specific optimization will be made in the SVM algorithm, the use of the RBF kernel gives better results than the linear kernel.[31] For this reason, RBF was used for the SVM algorithm. For the optimization of gamma and c values in this kernel, the Artificial Bee Colony algorithm, which is a heuristic optimization technique, was used.[32] When compared to other current heuristics, the Artificial Bee Colony algorithm is quite efficient for parameter optimization. Further, it is an easier method to understand and implement.[33]

Because the proposed method had two-level which performed both segmentation and classification, different metrics of the two processes were used in the model evaluation. In the segmentation process, since the number of hemorrhagic regions in an image can be more than one, the mAP value, which is an up-to-date instance segmentation metric, was used.[34] This value corresponds to the DICE score value in semantic segmentation.[34] At the same time, by applying 5-fold cross-validation, the segmentation process was re-evaluated to show that the proposed model is consistent. The fact that the mAP value obtained when random samples were taken, and the mAP values obtained as a result of cross-validation were similar showed that the segmentation was consistent across different data. In the evaluation of the classification process' success, the F1 score value was used together with the accuracy value. Especially in the case of unbalanced distribution among class labels, the accuracy parameter alone is not sufficient.[35-37] Since the F1 score increase indicates an increase in the model's success, the F1 score value is parallel to the accuracy value showing that the model is consistent. At the same time, the NPV value increase in the case of using SVM compared to using only Mask R-CNN clearly shows the model's success in detecting the hemorrhage absence. In addition, considering the FPR and FNR values used in the model's evaluation as a whole, the second level SVM model clearly reduced error.

Due to the lack of sufficient open data in the field of hemorrhagic areas detection from CT images and the need for time as well as physician expertise, especially in the segmentation process, there are a limited number of studies. However, some partial data sets that can be used in this area are present in the literature.[16,38,39] The first of these is the CQ500 data set.[16] This dataset contains 491 scans with 193317 slices of anonymized images labeled by three radiologists. However, these data do not have images unmasked for segmentation. The second contains two different datasets. One of them consists of 23409 CT images taken from the CQ500 dataset, which includes bounding box markings for five acute hemorrhage types. The other one has ground truth segmentation masks

as in our study. However, it has a limited number of data (56 slices) in terms of SDH.[38] The last one is a dataset containing more than 25,000 images created by American Neuroradiology Association and labeled by volunteers.[39] This dataset also does not have a ground truth segmentation mask. When all datasets were examined, it was determined that most of the CT images used did not have markings directly including the hemorrhagic region's borders, as images used in this study. Therefore, an open data set could not be used within the study's scope. For these reasons, first, labeling of CT images taken from 26 patients and exact marking of the hemorrhagic region's borders (obtaining ground truth data for segmentation) were provided.

In addition, to generalize the proposed model, slices containing only ASDH in the CQ500[16] dataset were marked to obtain the ASDH masks. After that, the model was retrained. When the obtained results were compared with the previous results, it was seen that there was a difference of about 1%, but the results were consistent. The reason for this difference is the low image quality of the scans in the CQ500. The images in the data set belong to 2017, so there is a clear quality difference between the collected data by us which belong to 2022. Despite this, the proposed model was able to perform both segmentation and classification with a similar accuracy rate on lower-quality images.

When the studies conducted in the past 5 years are examined, it has been observed that the DICE score value obtained without distinguishing the types of hemorrhages for the hemorrhagic region segmentation (considering the different data sets used) varies in the range of approximately 0.79–0.84.[40-42] The obtained values were generally calculated to give accuracy per patient (or per scan). When segmentation studies on types of hemorrhages are examined, it has been observed that segmentation of subdural hemorrhage is more difficult than others, and among subdural hemorrhage subtypes, segmentation of ASDH is more difficult than others.[43,44] Compared to other subacute and chronic subdural hemorrhages, the smaller area coverage of ASDHs often makes it difficult to detect. In the study performed by Xu *et al*., the DICE score value for subdural hemorrhage was obtained as approximately 0.82 (it is not clear how much of the study was ASDH), while in the study performed by Farzaneh *et al*., this value was obtained as approximately 0.67 for ASDH segmentation.[43,44] The literature shows that the DICE score value calculated in studies specific to ASDHs is decreased.[43,44] Within the study's scope, only ASDHs were studied, and the mAP value was obtained as approximately 0.75. Considering the studies in the literature for the detection of ASDHs, the obtained mAP value is at a level that can be considered really good.

Of the past 5 years in the literature, when the segmentation and hemorrhage detection studies are examined together, no study has been found that makes classification over the segmented region using 2 dimensional (2D) images, as in the proposed two-level model. Some studies were carried out solely to detect the presence of hemorrhage. In the study performed by Kumaravel *et al*., using the CQ500 open data set, the hemorrhage types were evaluated in general, and the presence or absence of hemorrhages was examined.[45] AlexNet, an old deep learning model, was used and a success rate of around 99% was achieved.[45] This shows that the images in the dataset are not very complex in terms of classification. When the studies on the data compiled specifically for the problem are examined, it has been determined that the success achieved with these data is relatively low.[24-28] In the study of Arbabshirani *et al*., in which they classified the data containing different hemorrhage types with 3D images as having or absent hemorrhage, the success was evaluated in the area under the curve value, and the accuracy was obtained as 84.6%.[46] The data set used in the study consists of CT images that have not been used in the previous studies and are not open access. In the binary classification made on 3D images by Remedios *et al*., the detection of the hemorrhage presence (images were classified as hemorrhage/no hemorrhage) was made using the precision value, and this value was obtained as 0.9698.[47] Patient-based accuracy values obtained in the studies performed by Arbabshirani *et al*. and Remedios *et al*. have a much higher accuracy when compared to the image-based accuracy values obtained in our study.[46,47] They studied images taken from the Vanderbilt University Medical Center, which is also not open access.[46,47] For each image in the dataset, the presence/absence of hemorrhage information is not available.[46,47] Our study, which is based on the segmentation of 2D images differs from the studies in the literature. In addition, the fact that CT generates image data mainly through the 2D image reconstruction shows that our method offers a more radical solution that is more suitable for the image acquisition method. Thus, data loss and workload that may occur due to 3D processing are eliminated. Aside from the fact that 3D image processing is not superior to our method, it is possible to create a 3D image from our marked outputs with simple image processing. In another study carried out by Phaphuangwittayakul *et al*., using a special data set, the success in detecting subdural hemorrhages for the classification process made on 3D images was achieved with 96.54% accuracy.[48] In the study, two open and one private data sets were used.[48] Images for different hemorrhage types were mixed in the datasets.[48] Classification of epidural, subdural, and intraparenchymal hemorrhage types has been made.[48] Subtypes of subdural hemorrhages have not been studied.[48] General subdural hemorrhage detection was made on the private data set.[48] In our study, ASDHs, which is one of the most difficult subdural hemorrhages, were detected with 96.36% accuracy on 2D images. Finally, Ye *et al*. classified hemorrhage types in terms of both binary (hemorrhage/no hemorrhage) and five hemorrhage types over the 3D CNN architecture.[49] Results are given on both patient and image basis.[49] The image-based accuracy for subdural hemorrhages was 94%, which is lower than the classification value we obtained in our study.[48] As stated in the literature, although

Table 4. Up-to-date list of studies on other intracranial hemorrhage types segmentation and classification*

Authors	Year	Segmentation/Classification	Method	Dataset
Chang *et al*.[64]	2018	Classification + Segmentation	Mask R-CNN (Deep Learning)	-
Cho et al.[65]	2019	Classification + Segmentation	CNN- and FCN-based architecture	Specific
Kyung et al.[66]	2019	Classification + Segmentation	FCN(Fully Convolutional Network) based architecture	Specific
Lee et al.[53]	2019	Classification + Segmentation	CNN-based architecture (Deep Learning)	Specific
Arab et al.[42]	2020	Segmentation	CNN-based architecture (Deep Learning)	Specific
Farzaneh et al.[44]	2020	Classification + Segmentation	Machine Learning	Specific
Yao et al.[67]	2020	Segmentation	CNN-based architecture (Deep Learning)	Open: PROTECT III trial
Heit et al.[68]	2021	Classification + Segmentation	hybrid 2D–3D architecture (RAPID ICH application-based)	Specific
Kellogg et al.[40]	2021	Segmentation	3D CNN-based architecture (Deep Learning)	Specific
Phaphuangwittayakul et al.[48]	2021	Classification + Segmentation	3D CNN-based architecture (Deep Learning)	Open: RSNA (Radiological Society of North America) 2019, PhysioNet, CMU-TBI (Carnegie Mellon University – Traumatic Brain Injury)
Sharrock et al.[69]	2021	Segmentation	3D Neural Network-based architecture	Specific
Solorio-Ramírez et al.[70]	2021	Classification + Segmentation	Minimalist Machine Learning	Open
Xu et al.[43]	2021	Segmentation	U-Net-based architecture (Deep Learning)	Specific
Zhao et al.[71]	2021	Segmentation	Unet-based architecture (Deep Learning)	Specific
Pandimurugan et al.[72]	2022	Classification + Segmentation	CNN + GAN(Generative Adversarial Networks) (Deep Learning)	Open: RSNA repositories data
Wang *et al*.[73]	2023	Segmentation	Capsule Network-based architecture	Specific

* All up-to-date (Last 5 years) related intracranial hematoma detection studies are given in the table in chronological and alphabetical order. The literature search was carried out in the PubMed database and "brain hemorrhage" deep learning, "brain hematoma" deep learning, "brain hemorrhage" machine learning, "brain hematoma" machine learning, "brain hematoma" segmentation classification, "brain hematoma" segmentation, "brain hemorrhage" segmentation classification, "brain hemorrhage" segmentation, "intracranial hematoma" segmentation classification, "intracranial hematoma" segmentation, "intracranial hemorrhage" segmentation classification, "intracranial hemorrhage" segmentation, "intracranial hemorrhage" artificial intelligence segmentation classification, and "intracranial hemorrhage" artificial intelligence segmentation keywords were used.

there is a need for detection studies about subdural hemorrhage subtypes,[48] there is no study conducted specifically for ASDHs except in our publication.

In addition to these studies, different machine learning (SVM,[50] clustering,[51] unsupervised learning,[52] etc.) techniques have been used for only classification purposes in the literature to detect cerebral hemorrhage. With the popularization of deep learning techniques, not only the classification problem but also the problem of detecting the hemorrhagic region has been focused on. For this purpose, generally, CNN,[53-55] Fully Convolutional. Networks,[56] Unet,[41] and ResNet[57,58] models have been preferred. And more recently, hybrid models (CNN + Long Short-Term Memory (LTSM),[55,59,60] Deep Learning + SVM,[57,61] Deep Learning + Deep Learning,[49,55,62] etc.) have been used. In most studies used datasets specific to the relevant study. Considering that currently there is no open data set suitable for segmentation, it would not be correct to make a superiority comparison between hybrid models. However, it can be said that deep learning based models and hybrid models are more successful than only machine learning based models.[63] In addition, the success of a single deep learning based model and the success of hybrid models may vary according to the problem and the model created.[55,57,61] For this reason, it would not be correct to make a direct superiority comparison among these techniques. For the aforementioned reasons, except for the studies that were compared in detail above, no comparison was made with the studies that did not contain any results in terms of subdural hemorrhages. Since extensive literature review of ASDHs already presented, studies including other types of brain hematomas and their features which are partially related our study is shown in detail in Table 4.

Finally, we would like to list the features that distinguish our work. As stated before when the literature is examined, it is seen that there are a limited number of studies that perform both classification and segmentation processes. Among those there was no study that performed the classification process over the segmented region. At the same time, studies were not carried out specifically on a subtype of ASDH. Rather, general models have been proposed to segment all hematoma types. Also, the data set used in many other studies were obtained specific (closed to public access) to the study. On the other hand, open datasets do not have a sufficient number of ground truth segmentation masks. Our study excels on those fronts and overall results.

Although we have planned our work as best we can, there are some shortcomings. Our most important shortcoming is the number of images reviewed. Although we have examined a good number of images compared to studies in the literature, due to the nature of the method we used, access to big data will give better results.[45-49] The most important reasons that prevent this from our point of view were the small number of researchers, scarcity of research centers, and our time constraints. Multicenter studies are needed. However, from our results, it is obvious that we have reached sufficient meaningful results. Another shortcoming is that we can only evaluate ASDHs for the same reasons. More articles will follow in terms of other pathologies, but it takes time with the available facilities. Finally, although our work has deeper technical details, we tried to explain it most optimally in the article format, so that everyone can understand it.

With this innovative study, we have obtained an ideal hybrid image processing method for ASDH detection, using a limited number of centers, researchers, and available resources. Compared to other studies, although our dataset is thought to be limited, we have a good dataset for ASDHs. In the project's continuation, we planned to develop algorithms that can identify other cranial traumas and create our final program. Thus, we think that a new deficiency created by the development of modern medicine has been filled with modern computer engineering techniques. We performed pathology determination in CT with our program, which has better negative and positive predictive values than today's interpretations with telemedicine techniques. Moreover, it frees us from today's delays and financial burdens.[21,22]

CONCLUSION

As proposed in the article, the two-level hybrid model provides automatic segmentation and classification of ASDHs on CT images. Our study aimed to support the medical diagnosis and treatment of ASDHs based on AI. For this purpose, through a single model, both the detection of hemorrhage and the presentation of the suspected area to the physician were provided. This process has been performed more successfully in existing telemedicine applications with low cost and high accuracy over 2D images. Thus, we presented the knowledge created by technology development in an easily understandable form and offered it to the service.

In future studies, it is aimed to develop specific models for other brain hemorrhage types and traumas to create a hybrid architecture that can handle the cranial pathologies as a whole.

Acknowledgment: Preparation for publication of this article is partly supported by the Turkish Neurosurgical Society in terms of English redaction. For their valuable contribution to the study, I would like to thank my esteemed teacher Prof. Dr. Ünal ÖZÜM, and my dear apprentice Dr. Zekeriya BULUT.

Ethics Committee Approval: Ethical consent for the study was obtained from the ethics committee of Sivas Republic University, Faculty of Medicine, non-interventional clinical studies, with the decision dated August 19, 2021 and numbered 2021–08/06. In addition, to explain that their anonymized data can be used within the ethical rules' framework, informed consents were obtained from all patients during hospital admissions.

Peer-review: Externally peer-reviewed.

Authorship Contributions: Concept: İ.K., F.K.G.; Design: İ.K., F.K.G.; Supervision: İ.K., F.K.G.; Resource: İ.K., F.K.G.; Materials: İ.K.; Data collection and/or processing: İ.K., F.K.G., T.H.G.; Analysis and/or interpretation: İ.K., F.K.G., T.H.G.; Literature search: F.K.G.; Writing: İ.K., F.K.G., T.H.G.; Critical review: İ.K., F.K.G., T.H.G.

Conflict of Interest: None declared.

Financial Disclosure: The authors declared that this study has received no financial support.

REFERENCES

1. Richmond C. Sir Godfrey Hounsfield. BMJ 2004;329:687. [CrossRef]
2. Kuno H, Sekiya K, Chapman MN, Sakai O. Miscellaneous and emerging applications of dual-energy computed tomography for the evaluation of intracranial pathology. Neuroimaging Clin N Am 2017;27:411–27. [CrossRef]
3. Hori K, Fujimoto T, Kawanishi K. Development of ultra-fast X-ray computed tomography scanner system. IEEE Trans Nucl Sci 1998;45:2089–94. [CrossRef]
4. What is an MRI scan and what can it do? Drug Ther Bull 2011;49:141-4. [CrossRef]
5. Endo M, Mori S, Kandatsu S, Tanada S, Kondo C. Development and performance evaluation of the second model 256-detector row CT. Radiol Phys Technol 2008;1:20-6. [CrossRef]
6. Howell JD. Early clinical use of the x-ray. Trans Am Clin Climatol Assoc 2016;127:341–9.
7. Brenner DJ, Hall EJ. Computed tomography--an increasing source of radiation exposure. N Engl J Med 2007;357:2277–84. [CrossRef]
8. Shuaib A, Jeerakathil T, Alberta Mobile Stroke Unit Investigators. The mobile stroke unit and management of acute stroke in rural settings. CMAJ 2018;190:E855–8. [CrossRef]
9. Health Statistics Türkiye. 2019 Health Statistics Yearbook for Türkiye; 2019 Available from: https://www.saglik.gov.tr/TR,84966/saglik-istatistikleri-yilligi-2019-yayinlanmistir.html. Accessed Mar 12, 2022.
10. Türkiye Ministry of Health Expert Board in Medicine. Türkiye Emergency Medicine Specialty Training Curriculum; 2022. Available from: https://tuk.saglik.gov.tr›aciltipmufredatv24doc. Accessed Mar 12, 2022.
11. Subramaniam RM, Kim C, Scally P. Medical student radiology teaching in Australia and New Zealand. Australas Radiol 2007;51:358–61. [CrossRef]
12. Wallis A, McCoubrie P. The radiology report--are we getting the message across? Clin Radiol 2011;66:1015–22. [CrossRef]
13. Kurzweil R. The Age of Intelligent Machines. Cambridge, Massachusetts MA: MIT Press; 1990.
14. Han J, Pei J, Kamber M. Data Mining: Concepts and Techniques. 3rd ed. Waltham, Massachusetts, MA: Elsevier; 2011.
15. Greenberg MS. Handbook of Neurosurgery. 9th ed. New York: Thieme; 2020. p. 408-53.
16. Publicly Available Dataset. Qure.ai.; 2018. Available from: https://headctstudy.qure.ai/#dataset. Accessed Mar 12, 2022.
17. Kerezoudis P, Goyal A, Puffer RC, Parney IF, Meyer FB, Bydon M. Morbidity and mortality in elderly patients undergoing evacuation of acute traumatic subdural hematoma. Neurosurg Focus 2020;49:E22. [CrossRef]
18. Karibe H, Hayashi T, Hirano T, Kameyama M, Nakagawa A, Tominaga T. Surgical management of traumatic acute subdural hematoma in adults: A review. Neurol Med Chir (Tokyo) 2014;54:887–94. [CrossRef]
19. Devos O, Ruckebusch C, Durand A, Duponchel L, Huvenne JP. Support vector machines (SVM) in near infrared (NIR) spectroscopy: Focus on parameters optimization and model interpretation. Chemometr Intell Lab Syst 2009;96:27–33. [CrossRef]
20. Langlois JA, Rutland-Brown W, Wald MM. The epidemiology and impact of traumatic brain injury: A brief overview. J Head Trauma Rehabil 2006;21:375–8. [CrossRef]
21. Alexander-Bates I, Neep MJ, Davis B, Starkey D. An analysis of radiographer preliminary image evaluation - A focus on common false negatives. J Med Radiat Sci 2021;68:237–44. [CrossRef]
22. Grieve FM, Plumb AA, Khan SH. Radiology reporting: A general practitioner's perspective. Br J Radiol 2010;83:17–22. [CrossRef]
23. Chamley RR, Holdsworth DA, Rajappan K, Nicol ED. ECG interpretation. Eur Heart J 2019;40:2663–6. [CrossRef]
24. Dogan RO, Dogan H, Bayrak C, Kayikcioglu T. A two-phase approach using mask R-CNN and 3D U-Net for high-accuracy automatic segmentation of pancreas in CT imaging. Comput Methods Programs Biomed 2021;207:106141. [CrossRef]
25. Fudickar S, Nustede EJ, Dreyer E, Bornhorst J. Mask R-CNN Based *C. elegans* detection with a DIY microscope. Biosensors (Basel) 2021;11:257. [CrossRef]
26. Lee HH, Kwon BM, Yang CK, Yeh CY, Lee J. Measurement of laryngeal elevation by automated segmentation using Mask R-CNN. Medicine (Baltimore) 2021;100:e28112. [CrossRef]
27. Zhang J, Cosma G, Watkins J. Image enhanced mask R-CNN: A deep learning pipeline with new evaluation measures for wind turbine blade defect detection and classification. J Imaging 2021;7:46. [CrossRef]
28. Zhang Y, Chan S, Park VY, Chang KT, Mehta S, Kim MJ, et al. Automatic detection and segmentation of breast cancer on MRI using mask R-CNN trained on non-fat-sat images and tested on fat-sat images. Acad Radiol 2022;29 Suppl 1:S135–44. [CrossRef]
29. Kuo BC, Ho HH, Li CH, Hung CC, Taur JS. A kernel-based feature selection method for SVM with RBF kernel for hyperspectral image classification. IEEE J Sel Top Appl Earth Obs Remote Sens 2014;7:317–26. [CrossRef]
30. Nguyen QH, Nguyen BP, Nguyen TB, Do TT, Mbinta JF, Simpson C. Stacking segment-based CNN with SVM for recognition of atrial fibrillation from single-lead ECG recordings. Biomed Sig Process Control 2021;68:102672. [CrossRef]
31. Keerthi SS, Lin CJ. Asymptotic behaviors of support vector machines with Gaussian kernel. Neural Comput 2003;15:1667–89. [CrossRef]
32. Karaboga D, Basturk B. A powerful and efficient algorithm for numerical function optimization: Artificial bee colony (ABC) algorithm. J Glob Optim 2007;39:459–71. [CrossRef]
33. Zahedi L, Mohammadi FG, Amini MH. HyP-ABC: A Novel Automated Hyper-Parameter Tuning Algorithm Using Evolutionary Optimization. arXiv:210905319 [cs]; 2021. Available from: https://arxiv.org/abs/2109.05319. Accessed Mar 13, 2022. [CrossRef]
34. Vuola AO, Akram SU, Kannala J. Mask-RCNN and U-net Ensembled for Nuclei Segmentation. arXiv:190110170 [cs]; 2019. Available from: https://arxiv.org/abs/1901.10170. Accessed Mar 12, 2022.
35. Tuncer SA, Çınar A, Fırat M. Hybrid CNN based computer-aided diagnosis system for choroidal neovascularization, diabetic macular edema, drusen disease detection from OCT images. Traitement Sig 2021;38:673–9. [CrossRef]
36. Pandey M, Jha B, Thakur R. An exploratory analysis pertaining to stress detection in adolescents. In: Advances in Intelligent Systems and Computing. Berlin: Springer; 2020. p. 413–21. [CrossRef]
37. Jin X, Jie L, Wang S, Qi HJ, Li SW. Classifying wheat hyperspectral pixels of healthy heads and fusarium head blight disease using a deep neural network in the wild field. Remote Sens 2018;10:395. [CrossRef]

38. Goldberger AL, Amaral LA, Glass L, Hausdorff JM, Ivanov PC, Mark RG, et al. PhysioBank, PhysioToolkit, and PhysioNet: Components of a new research resource for complex physiologic signals. Circulation 2000;101:E215–20. [CrossRef]
39. RSNA Intracranial Hemorrhage Detection Dataset. Kaggle; 2019. Available from: https://www.kaggle.com/c/rsna-intracranial-hemorrhage-detection/data [Last accessed on 2022 Mar 12].
40. Kellogg RT, Vargas J, Barros G, Sen R, Bass D, Mason JR, et al. Segmentation of chronic subdural hematomas using 3D convolutional neural networks. World Neurosurg 2021;148:e58–65. [CrossRef]
41. Li L, Wei M, Liu B, Atchaneeyasakul K, Zhou F, Pan Z, et al. Deep learning for hemorrhagic lesion detection and segmentation on brain CT images. IEEE J Biomed Health Inform 2021;25:1646–59. [CrossRef]
42. Arab A, Chinda B, Medvedev G, Siu W, Guo H, Gu T, et al. A fast and fully-automated deep-learning approach for accurate hemorrhage segmentation and volume quantification in non-contrast whole-head CT. Sci Rep 2020;10:19389. [CrossRef]
43. Xu J, Zhang R, Zhou Z, Wu C, Gong Q, Zhang H, et al. Deep Network for the automatic segmentation and quantification of intracranial hemorrhage on CT. Front Neurosci 2021;14:541817. [CrossRef]
44. Farzaneh N, Williamson CA, Jiang C, Srinivasan A, Bapuraj JR, Gryak J, et al. Automated segmentation and severity analysis of subdural hematoma for patients with traumatic brain injuries. Diagnostics (Basel) 2020;10:773. [CrossRef]
45. Kumaravel P, Mohan S, Arivudaiyanambi J, Shajil N, Venkatakrishnan HN. A simplified framework for the detection of intracranial hemorrhage in CT brain images using deep learning. Curr Med Imaging 2021;17:1226–36. [CrossRef]
46. Arbabshirani MR, Fornwalt BK, Mongelluzzo GJ, Suever JD, Geise BD, Patel AA, et al. Advanced machine learning in action: Identification of intracranial hemorrhage on computed tomography scans of the head with clinical workflow integration. NPJ Digit Med 2018;1:9. [CrossRef]
47. Remedios SW, Wu Z, Bermudez C, Kerley CI, Roy S, Patel MB, et al. Extracting 2D weak labels from volume labels using multiple instance learning in CT hemorrhage detection. Proc SPIE Int Soc Opt Eng 2020;11313:10.1117/12.2549356. [CrossRef]
48. Phaphuangwittayakul A, Guo Y, Ying F, Dawod AY, Angkurawaranon S, Angkurawaranon C. An optimal deep learning framework for multi-type hemorrhagic lesions detection and quantification in head CT images for traumatic brain injury. Appl Intell (Dordr) 2021;52: 7320–38. [CrossRef]
49. Ye H, Gao F, Yin Y, Guo D, Zhao P, Lu Y, et al. Precise diagnosis of intracranial hemorrhage and subtypes using a three-dimensional joint convolutional and recurrent neural network. Eur Radiol 2019;29:6191–201. [CrossRef]
50. Shahangian B, Pourghassem H. Automatic brain hemorrhage segmentation and classification algorithm based on weighted grayscale histogram feature in a hierarchical classification structure. Biocybern Biomed Eng 2016;36:217–32. [CrossRef]
51. Singh P, Khanna V, Kamal M. Hemorrhage Segmentation by Fuzzy C-Mean with Modified Level Set on CT Imaging. In: 5th International Conference on Signal Processing and Integrated Networks (SPIN); 2018. p. 550–5. [CrossRef]
52. Mohadikar P, Duan Y, Carr S. Brain Intracranial Hemorrhage Segmentation using Unsupervised Learning on Volume CT Images. Conference. In: IEEE Applied Imagery Pattern Recognition Workshop (AIPR); 2021. p. 1–5. [CrossRef]
53. Lee H, Yune S, Mansouri M, Kim M, Tajmir SH, Guerrier CE, et al. An explainable deep-learning algorithm for the detection of acute intracranial haemorrhage from small datasets. Nat Biomed Eng 2019;3:173–82. [CrossRef]
54. Vrbančič G, Zorman M, Podgorelec V. Transfer Learning Tuning Utilizing Grey Wolf Optimizer for Identification of Brain Hemorrhage from Head CT Images. In: Book: StuCoSReC. Proceedings of the 2019 6th Student Computer Science Research Conference; 2019. p. 61–6. [CrossRef]
55. Mushtaq MF, Shahroz M, Aseere AM, Shah H, Majeed R, Shehzad D, et al. BHCNet: Neural network-based brain hemorrhage classification using head CT scan. IEEE Access 2021;9:113901–16. [CrossRef]
56. Kuo W, Häne C, Yuh E, Mukherjee P, Malik J. Cost-Sensitive Active Learning for Intracranial Hemorrhage Detection. arXiv:180902882 [cs]; 2018. Available from: https://arxiv.org/abs/1809.02882. Accessed Dec 15, 2022.
57. Titano JJ, Badgeley M, Schefflein J, Pain M, Su A, Cai M, et al. Automated deep-neural-network surveillance of cranial images for acute neurologic events. Nat Med 2018;24:1337–41. [CrossRef]
58. Lewick T, Kumar M, Hong R, Wu W. Intracranial Hemorrhage Detection in CT Scans using Deep Learning. IEEE Xplore. Oxford, UK: IEEE, 2020, pp. 169–72. [CrossRef]
59. Ko H, Chung H, Lee H, Lee J. Feasible study on intracranial hemorrhage detection and classification using a CNN-LSTM network. Annu Int Conf IEEE Eng Med Biol Soc 2020;2020:1290–3. [CrossRef]
60. Patel A, van de Leemput SC, Prokop M, Van Ginneken B, Manniesing R. Image level training and prediction: Intracranial hemorrhage identification in 3D non-contrast CT. IEEE Access 2019;7:92355–64. [CrossRef]
61. Dawud AM, Yurtkan K, Oztoprak H. Application of deep learning in neuroradiology: Brain haemorrhage classification using transfer learning [published correction appears in Comput Intell Neurosci 2020;2020:4705838]. Comput Intell Neurosci 2019;2019:4629859. [CrossRef]
62. Guo D, Wei H, Zhao P, Pan Y, Yang HY, Wang X, et al. Simultaneous Classification and Segmentation of Intracranial Hemorrhage Using a Fully Convolutional Neural Network. USA: IEEE Xplore; 2020, pp. 118–21. [CrossRef]
63. Dargan S, Kumar M, Ayyagari MR, Kumar G. A survey of deep learning and its applications: A new paradigm to machine learning. Arch Comput Methods Eng 2020;27:1071–92. [CrossRef]
64. Chang PD, Kuoy E, Grinband J, Weinberg BD, Thompson M, Homo R, et al. Hybrid 3D/2D convolutional neural network for hemorrhage evaluation on head CT. AJNR Am J Neuroradiol 2018;39:1609–16. [CrossRef]
65. Cho J, Park KS, Karki M, Lee E, Ko S, Kim JK, et al. Improving sensitivity on identification and delineation of intracranial hemorrhage lesion using cascaded deep learning models. J Digit Imaging 2019;32:450–61. [CrossRef]
66. Kyung S, Shin K, Jeong H, Kim KD, Park J, Cho K, et al. Improved performance and robustness of multi-task representation learning with consistency loss between pretexts for intracranial hemorrhage identification in head CT. Med Image Anal 2022;81:102489. [CrossRef]
67. Yao H, Williamson C, Gryak J, Najarian K. Automated hematoma segmentation and outcome prediction for patients with traumatic brain injury. Artif Intell Med 2020;107:101910. [CrossRef]
68. Heit JJ, Coelho H, Lima FO, Granja M, Aghaebrahim A, Hanel R, et al. Automated cerebral hemorrhage detection using RAPID. AJNR Am J Neuroradiol 2021;42:273–8. [CrossRef]
69. Sharrock MF, Mould WA, Ali H, Hildreth M, Awad IA, Hanley DF, et al. 3D deep neural network segmentation of intracerebral hemorrhage: Development and validation for clinical trials. Neuroinformatics 2021;19:403–15. [CrossRef]
70. Solorio-Ramírez JL, Saldana-Perez M, Lytras MD, Moreno-Ibarra MA, Yáñez-Márquez C. Brain hemorrhage classification in CT scan images using minimalist machine learning. Diagnostics (Basel) 2021;11:1449. [CrossRef]
71. Zhao X, Chen K, Wu G, Zhang G, Zhou X, Lv C, et al. Deep learning shows good reliability for automatic segmentation and volume measurement of brain hemorrhage, intraventricular extension, and peripheral edema. Eur Radiol 2021;31:5012–20. [CrossRef]
72. Pandimurugan V, Rajasoundaran S, Routray S, Prabu AV, Alyami H, Alharbi A, et al. Detecting and extracting brain hemorrhages from CT images using generative convolutional imaging scheme. Comput Intell Neurosci 2022;2022:6671234. [CrossRef]
73. Wang L, Tang M, Hu X. Evaluation of grouped capsule network for intracranial hemorrhage segmentation in CT scans. Sci Rep 2023;13:3440. [CrossRef]

ORİJİNAL ÇALIŞMA - *ÖZ*

İki katmanlı yapay zeka modeline dayalı devrimsel akut subdural hematom tespiti

Dr. İsmail Kaya,[1] Dr. Tuğrul Hakan Gençtürk,[2] Dr. Fidan Kaya Gülağız[2]

[1]Niğde Ömer Halisdemir Üniversitesi, Tıp Fakültesi, Beyin ve Sinir Cerrahisi Anabilim Dalı, Niğde, Türkiye
[2]Kocaeli Üniversitesi, Mühendislik Fakültesi, Bilgisayar Mühendisliği Anabilim Dalı, Kocaeli, Türkiye

AMAÇ: Bu çalışmayı, beyin tomografisinin yorumlanmasında doğruluk ve süre açısından gördüğümüz eksikliklerin yapay zeka (AI) yöntemi ile doldurularak en azından sorumlu doktoru hızlıca uyaracak şekilde, uygun patolojilerde yardımcı olabileceğini düşünüp akut subduraller açısından ilk değerlendirmeyi yapmak için planladık.
GEREÇ ve YÖNTEM: İki seviyeli AI tabanlı bir hibrit yöntem geliştirildi. Önerilen model, hemorajik bölgenin maske oluşturma aşamasında bir derin öğrenme modeli olan maske-bölge evrişimli sinir ağı (Mask R-CNN) tekniğini ve ikili sınıflandırma aşamasında bir makine öğrenimi modeli olan probleme özel, optimize edilmiş destek vektör makineleri (SVM) tekniğini kullanır. Ayrıca SVM algoritmalarının parametrelerinin optimizasyonu için arı kolonisi algoritması kullanıldı.
BULGULAR: İlk aşamada kullanılan Mask R-CNN mimarisi ile kesişim üzeri birleşme (IOU) değeri 0.5 alındığında ortalama ortanca kesinlik (mAP) değeri 0.754 olarak elde edildi. Aynı zamanda 5 kat çapraz doğrulama uygulandığında mAP değeri 0.736 olarak elde edildi. Hem Mask R-CNN hem de SVM algoritması için hiper parametre optimizasyonu ile iki seviyeli sınıflandırma işleminin doğruluğu %96.36 idi. Ayrıca nihai yanlış negatif oran ve yanlış pozitif oran değerleri sırasıyla %6.20 ve %2.57 olarak elde edildi.
SONUÇ: Önerilen model ile iki boyutlu görüntüler üzerinde hem kanama tespiti hem de şüpheli alanın hekime sunulması, benzer çalışmalara ve günümüz tele tıp teknikleri ile yorumlamalara göre düşük maliyet ve yüksek doğrulukla daha başarılı bir şekilde gerçekleştirilmiştir.
Anahtar sözcükler: Yapay zeka; akut subdural hematom; erken tanı.

Ulus Travma Acil Cerrahi Derg 2023;29(8):858-871 DOI: 10.14744/tjtes.2023.76756